Int. J. Morphol.,
42(5):1312-1321, 2024.

Effects of Apricot Kernel Oil Extract on the Cognitive Function and Expression Profile of Inflammatory Factors in a Rat Model of Hemorrhagic Stroke: A Biochemical, Immunohistochemical and Molecular Approach

Efectos del Extracto de Aceite de Semilla de Albaricoque sobre la Función Cognitiva y el Perfil de Expresión de Factores Inflamatorios en un Modelo de Accidente Cerebrovascular Hemorrágico en Ratas: Un Enfoque Bioquímico, Inmunohistoquímico y Molecular

Dengpan Hong[1]; Lijie Bi[2]; Feng Qiang[3]; Xiao Chen[4] & Weiping Qiang[5]

HONG, D.; BI, L.; QIANG, F.; CHEN, X. & QIANG , W. Effects of Apricot kernel oil extract on the cognitive function and expression profile of inflammatory factors in a rat model of hemorrhagic stroke: A biochemical, immunohistochemical and molecular approach. *Int. J. Morphol., 42(5)*:1312-1321, 2024.

SUMMARY: Cerebral hemorrhage (CH) presents a significant risk for cognitive decline. Our research aimed to assess the impact of Apricot Kernel Oil (AKO) on cognitive function and inflammatory response in a hemorrhagic stroke model using Wistar rats, and to examine their correlation. Fifty Wistar rats were randomly assigned to five groups: a control group, an AKO supplemented group (receiving 400 mg/kg AKO), a CH group (with induced CH), and CH groups supplemented with 200 and 400 mg/kg AKO, each containing 10 rats. Cognitive function was evaluated using the Y-electric maze test across these groups. Additionally, enzyme-linked immunosorbent assay and real-time PCR were utilized to analyze the protein and gene expression profiles of inflammatory and apoptotic factors in the brain. Compared to the control group, rats in the CH group took longer to master the maze criteria ($P<0.05$). Moreover, the CH group exhibited significantly increased levels of pro-inflammatory cytokines interleukin-1β (IL-1β), IL-6, and tumor necrosis factor-α, and decreased levels of anti-inflammatory cytokines IL-4 and IL-10 compared to the control group ($P<0.05$). Conversely, rats in the CH+400 mg/kg AKO group showed opposite trends in electrical simulation time, inflammatory factor protein, and gene expression profile (Bcl-2, BAX, Caspase-3, and p53) compared to the CH group ($P<0.05$). Our findings suggest that AKO extract may ameliorate cognitive dysfunction following CH in rats, potentially through modulation of inflammatory factors secreted by microglia.

KEY WORDS: Apricot kernel oil; Inflammation; Apoptosis; Cerebral hemorrhage.

INTRODUCTION

Cerebral hemorrhage (CH), also known as intracerebral hemorrhage, is a stroke resulting from bleeding within brain tissue, causing severe neurological damage and significant global morbidity and mortality. The incidence is approximately 24 per 100,000 person-years, higher in low- and middle-income countries, and increases with age, especially affecting those over 55 (Wang *et al*., 2022). Major risk factors include hypertension, anticoagulant therapy, cerebral amyloid angiopathy, smoking, alcohol use, and genetic predispositions. Secondary damage from CH and reperfusion injury often leads to neuronal dysfunction and cell death, resulting in cognitive impairments, disability, or fatality. Without prompt treatment, neurons in the ischemic penumbra can rapidly die due to overproduction of free radicals and a massive inflammatory response (Magid-Bernstein *et al*., 2022). Pro-inflammatory cytokines like IL-1β can trigger detrimental NF-κB nuclear translocation and increase p53-upregulated modulators of apoptosis, causing neuronal apoptosis and brain injury. Post-ischemic cytokines, including TNF-α, degrade the microenvironment of new

[1] Seven Departments of Encephalopathy, Xi'an TCM Hospital of Encephalopathy, Xi'an, 710032, China.
[2] Department of Intensive Care Unit, Xi'an TCM Hospital of Encephalopathy, Xi'an, 710032, China.
[3] Department of Traditional Chinese Medicine, Yan'an University Xianyang Hospital, Xian'yang, 711200, China.
[4] Nine departments of encephalopathy, Xi'an TCM Hospital of Encephalopathy, Xi'an, 710032, China
[5] Two Departments of Encephalopathy, Xi'an TCM Hospital of Encephalopathy, Xi'an, 710032, China.

Received: 2024-06-28 Accepted: 2024-07-07

neurons (Deng *et al*., 2021). Despite advances in understanding CH and cerebral ischemia at various levels, therapeutic options remain challenging due to serious drug side effects, a very short therapeutic window (≤3 hours post-CH), and secondary damage from CH and reperfusion injury (Zeng *et al*., 2021).

Interest in traditional herbal medicines has been growing, recognizing their potential in drug development due to their multi-target abilities, good synergy, and holistic approach, which offer advantages over the single target-single compound methods (Duan *et al*., 2022). Apricot kernel, derived from the seed inside the *Prunus armeniaca* L. fruit, has traditionally been used to treat cardiovascular disorders, diarrhea, anorexia, and skin lesions. Apricot kernel oil (AKO), rich in proteins, vitamins, carbohydrates, and minerals, is utilized in food products, antimicrobial films, and quality oil production. LC-ESI-MS/MS analysis reveals that AKO contains isoflavonoids like daidzein and luteolin, flavonoids such as apigenin and quercetin, saponins, carotenoids, essential fatty acids, anthocyanins, and amygdalin derivatives. Predominantly used in Asia, especially China, AKO is effective in treating ischemic heart diseases, providing anti-anginal effects, and enhancing antioxidant and anti-inflammatory responses as well as coronary flow velocity (Akhone *et al*., 2022).

Studies show that AKO can prevent acute myocardial infarction in rats by reducing infarct size and suppressing myocardial cell apoptosis (Jaafar, 2021). AKO exhibits anti-inflammatory and anti-apoptotic effects by inhibiting interleukin-6 (IL-6) and tumor necrosis factor alpha (TNF-α). This leads to the downregulation of nuclear factor kappa B (NF-κB) expression and modulation of the apoptotic pathway, which is dependent on mitogen-activated protein kinases (MAPKs) and the phosphoinositide-3-kinase–protein kinase B/Akt (PI3K-PKB/Akt) signaling pathways (Zhang *et al*., 2017a). Flavonoids in AKO, including apigenin, quercetin, and daidzein, are primarily responsible for reducing inflammation and pain related to central nervous system diseases (Akhone *et al*., 2022). They achieve this by inhibiting the activity of cyclooxygenase-2 and lipoxygenase, key enzymes involved in the inflammatory cascade (Charalabopoulos *et al*., 2019). Pharmacokinetic studies confirm that seven compounds from AKO are absorbed into the bloodstream following oral administration in rats. This study aims to further investigate which bioactive compounds reach injured brain tissue and contribute to brain protection after AKO extract administration (Jangdey *et al*., 2018). The neuroprotective effects of AKO pretreatment were examined, particularly focusing on its anti-apoptotic and anti-inflammatory properties, using the Morris water maze to assess its impact on rat brain function.

MATERIAL AND METHOD

Preparation of AKO: The freshly apricot kernel (4000 g) underwent drying at 38 °C in a dark environment, following confirmation by a botanist. Subsequently, the kernels were pulverized using a soil grinder, yielding a powder, which was then combined with ethanol/acetone (50:50 v/v). After incubation (38 °C/48 h), the mixture underwent filtration through a paper filter, followed by compression using a rotary evaporator. The resulting extract (325 grams) was maintained at 4°C (Gomaa, 2013).

Experimental design: Fifty male Wistar rats, with (195±15 g), were randomly allocated into 5 groups (n=10 per group). Prior to commencing the study, a 72-hour adaptation period was provided for the rats to acclimate to the study conditions, including temperature, food, and water. The rats were housed in propylene cages kept at 23±4 °C, with a relative humidity of 35±5 %, and subjected to a 12/12 dark/light cycle. They had access to standard pellets and tap water. All procedures related to the care and euthanasia of the rats were conducted under the oversight and approval of the ethics committee at Xi'an TCM hospital of encephalopathy ethics committee, adhering strictly to established protocols for the housing and handling of laboratory animals. The healthy control group was treated with intraperitoneal injection of 0.5 ml PBS, while the CH group received a single intracerebral injection with a stereotaxic apparatus of 0.5 µl/rat collagenase in right hippocampus. The co-treatment groups (CH +200 and CH +400 AKO) were orally administered collagenase along with 200 and 400 mg/kg of AKO, respectively. Furthermore, the healthy+400 AKO group received 400 mg/kg of AKO orally. The LD_{50} technique was employed to determine the effective dose of the non-toxic treatment, along with preliminary studies and existing research on collagenase and AKO. Administration of AKO occurred daily at fixed times (9 am) for 50 days (Tian *et al*., 2016; Zhang *et al*., 2017b).

LD_{50} for AKO. The LD_{50} of AKO was determined using Lork's two-step method. First, nine animals were allocated to three groups and administered AKO at 20, 200, and 2000 mg/kg, respectively. Subsequently, these rats were closely observed for any signs of mortality or toxicity within 24 hours. Following this, another set of three rats per group received AKO at 100, 500, and 5000 mg/kg, and similarly monitored within the same timeframe. The LD50 was calculated utilizing Lork's formula, incorporating the lowest dose and the highest safe dose (D safe) resulting in mortality (toxic dose, D toxic) observed during the monitoring period.

$$LD_{50} = (D\ safe \times D\ toxic)\ 1/2$$ (Wang *et al*., 2023).

Morris water maze test. The Morris water maze is widely used as an assessment of spatial learning and memory (Morris *et al*., 1982), and it was applied in this study from day 20 to 40 after CH. In brief, the water maze device consisted of a circular water tank (120 cm in diameter and 50 cm in depth) in a dark and quiet room with several prominent visual cues. The water temperature was maintained at 25 ± 1°C. A black rounded platform (10 cm in diameter) was submerged 2.0 cm below the surface of the water in the center of the quadrant and stayed in the same position during the training period. Rats' swimming trajectories were recorded by a video camera with a computer, and the parameters were sent to an image analyzer.

Each rat was trained twice per day for five consecutive days. For every trail, the rat was placed into the water facing the wall of the pool from four starting points in a different order and allowed to swim. The time to reach the hidden platform (escape latency) was measured for up to 90 s. If the rat failed, it would be guided to find the platform and allowed to remain there for 15 s, and their escape latency was recorded as 90 s. Finally, 24 h after the last training day, the platform was removed and the rats were tested on a 90-s retention probe trial. The number of times the rats crossed the position where the platform had previously been located was also recorded during the 90-s trail (Zhang *et al*., 2017a).

Glutathione peroxidase (GPx), Catalase (CAT), and Superoxide dismutase (SOD) serum activity. We utilized a sandwich-based ELISA kit specifically designed for rodents, sourced from Cusabio company in China, to quantify the serum activity of GPx (Cat. No.: CSB-E12146r), CAT (Cat. No.: CSB-E13439r), and SOD (Cat. No.: CSB-EL022397RA), as instructed (Wang *et al*., 2023).

Serum levels of nitric oxide (NO). The Griess colorimetric approach evaluated serum NO levels, which serve as crucial indicators of lipid peroxidation (LPO) and oxidative stress (OS). In summary, 500 µl of serum specimens were mixed with 6 mg of zinc oxide, thoroughly combined, and then centrifuged at 10,000 g for 15 min. The resulting supernatant was added to Griess solution (500 µl). Following incubation for 60 min at 37 °C, the mixture absorbance was measured using a Stat Fax ELISA reader (303 microwell readers, Awareness Technology company, United States) at wavelengths of 540 nm and 630 nm (Tsai *et al*., 2021).

Liver tissue LPO levels (TBARS levels), total antioxidant capacity (FRAP levels), and thiol levels. One method utilized to assess total antioxidant capacity involves FRAP evaluation. In brief, 100 mg of brain tissue was homogenized at 4 °C and then mixed with cold PBS (200 µl). From this mixture, 100 µl was transferred to 10 µl of FRAP solution. Following an incubation period of 15 minutes at 25 °C and subsequent centrifugation (12,000 g / 10 min), the supernatant absorbance was assessed at 593 nm by a Stat Fax ELISA reader (303 microwell readers, Awareness Technology Company, United States).

Another method to measure LPO levels involves assessing TBARS in brain tissue. Initially, the homogenized intestinal tissue mixture (100 µl) was mixed with TBARS solution (100 µl), and then underwent incubation at 37°C for 30 minutes and centrifugation (12,000 g / 5 min). The supernatant absorbance was then assessed at 593 nm by an ELISA reader.

To determine thiol levels in brain tissue, an important tissue antioxidant indicator, 100 µl of homogenized intestinal tissue mixture was combined with 5,5-dithio-bis-(2-nitrobenzoic acid) (DTNB; 20 µl), followed by incubation at 37°C for 15 min and centrifugation (12,000 g / 5 min). The supernatant absorbance was assessed at 412 nm by an ELISA reader (Zhang *et al*., 2017b; Wang *et al*., 2023).

Serum concentrations of TNF-α, IL-1β, IL-10, and IL-6. To assess the anti-inflammatory properties of VAFE extract, levels of pro-inflammatory cytokines [IL-6 (Cat. No.: M6000B), TNF-α (Cat. No.: NBP2- DY410), and IL-1β (Cat. No.: RLB00)], and the anti-inflammatory cytokine IL-10 (Cat. No.: R1000), were quantified using sandwich-oriented rodent-specific ELISA kits obtained from Novus Biologicals (United States) as instructed (Fouad *et al*., 2020).

IL-1β, IL-6, TNF-α, and p53 genes expression. Total RNA was extracted using Trizol following the instructions provided by the manufacturer (Ambion, China). Subsequently, 5 µg of total RNA was reverse transcribed into cDNA using random primers. Quantitative real-time PCR was carried out using SYBR Green (Vazyme, China) on a fluorescence real-time PCR detection system (ABI7900, CA, USA) under the following PCR reaction conditions: 50 °C for 2 min; 95 °C for 10 min; 95 °C for 30 s; 60 °C for 30 s; 40 cycles. Table I lists the primers utilized in this study. The gene expression was normalized to GAPDH expression. Relative expression levels of the genes were determined utilizing the threshold cycle (Ct) of all genes, ΔΔCt, and the fold change formula.

The fold formula change = $2^{-\Delta\Delta CT}$; ΔΔCt = [(Ct sample - Ct GAPDH gene) - (Ct sample – Ct control)] (Hassan *et al*., 2021).

Expression IL-1β, IL-6, TNF-α, and p53 proteins in brain with western blotting. The samples were lysed in RIPA buffer that contained protease and phosphatase

inhibitors for 30 min. The protein concentration was assessed using a BCA protein assay kit (Beyotime, China). Then, 40 μg of protein was separated on a 10 % SDS–polyacrylamide gel through electrophoresis and transferred to a PVDF membrane. The membranes were closed with a closure solution [5 % (w/v) skim milk powder] for 1 h and then incubated overnight at 4 °C with the following antibodies from Abcam, UK: anti- IL-1β (Cat. No. ab9722; 1:300), anti-IL-6 (Cat. No. ab6672; 1:200), anti-TNF-α (Cat. No. ab220210; 1:200), and anti-p53 (Cat. No. ab154036; 1:200). After three thorough washes with PBST, the membranes were exposed to the HRP-conjugated secondary antibody (1:5000) for 1 h. The bands were visualized using ECL (Amersham Pharmacia Biotech, Piscataway, NJ), and their intensity was quantified using Image J gel analysis software. All experiments were conducted three times (Hassan *et al*., 2021).

Table I. Primer sequences.

Gene	Sequences (5'–3')
GAPDH	F: TGAAGGTCGGAGTCAACGG
	R: AGAGTTAAAAGCAGCCCTGGTG
IL-6	F: GCCCTTCAGGAACAGCTATG
	R: TGTCAACAACATCAGTCCCAAGA
IL-1β	F: GCAACTGTTCCTGAACTCAACT
	R: ATCTTTTGGGGTCCGTCAACT
TNF-α	F: CCCACGTCGTAGCAAACCACCAA
	R: GGGATGAACCAGGGTCTGGGCC
P53	F: GGAAGACAGGCCCAGACTAT
	R: GCTCGACGCTAGGATCTGAC

Immunohistochemistry (IHC) assay. Paraffin sections of 3 μm thickness underwent deparaffinization and dehydration with an ethanol gradient. Afterward, the sections were exposed to 3 % H_2O_2 to eliminate endogenous peroxidase. They were then incubated with an anti- p53 (1:500; Cat. No.: GAF1355) antibody (R&D Systems, Inc., US) at 4 °C overnight. Following this, the sections were incubated with HRP-conjugated secondary antibodies at 37 °C for 30 min. The sections were then stained with hematoxylin and sealed, and images were acquired. A BX61TRF optical microscope (Olympus, Japan), attached to Image J software, facilitated the examination of the slides at a magnification of 400X. Following counting p53-positive cells in 10 fields of view in 400X and calculating the p53-positive cells / the total cells ratio, the percentage of p53 expression was determined (Zhang *et al*., 2017a).

Brain histopathology. Brain tissues were treated with 4 % paraformaldehyde for fixation, followed by being embedded in paraffin and cut into 3 μm thick sections utilizing a microtome (Model No. SM2010RV1.2 microtomes, LEICA, Germany). Subsequently, the sections were deparaffinized and rehydrated using an ethanol gradient. Hematoxylin and eosin (H&E) staining was performed on the sections. A light microscope performed histological analysis of the slides at ×400 magnifications. The images were captured employing a BX61TRF calibrated light microscopic system (Olympus, Japan) and processed using ImageJ software.

Statistical analysis. was carried out with the use of GraphPad Prism 7.0 (San Diego, CA, USA). The data are shown as the mean ± SD and analyzed by the one-way analysis of variance (ANOVA). Statistical significance was defined as a p value less than 0.05.

RESULTS

LD_{50} of AKO. Following a 24-hour observation of the groups subjected to AKO treatment, the outcomes indicated the identification of a safe dose (D safe) at 2000 mg/kg, with the toxic dose (D toxic) established at 5000 mg/kg of AKO. Employing Lork's formula, the calculated LD50 for AKO was determined to be 3162 mg/kg. This implies that animal studies can utilize doses lower than the LD50 of AKO.

AKO improved CH-induced spatial cognitive deficits. To investigate the effect of chronic CH and AKO treatment on cognitive function, we exposed the animal to the Morris water maze test after 50 days of treatment. All rats exhibited a progressively shorter escape latency in a day-dependent manner by training every day, and there was an obviously differences among groups. One-way ANOVA showed that, beginning on day 4, animals in the healthy group demonstrated a shorter latency to finding the platform compared with those in the CH group ($p < 0.05$), and the results were similar on day 5 ($p < 0.05$). These data clearly show the impairment of memory by CH. The escape latency was greatly decreased on day 4 ($p < 0.05$) and day 5 ($p < 0.05$) after CH+400 AKO treatment. Although it was not statistically significant, CH+200 AKO treatment also rendered shorter escape latencies than the CH group ($p > 0.05$). These results indicated that CH+400 AKO treatment effectively ameliorated spatial learning through 5-day training. As shown in Figure 1, in the probe test without the platform, CH-rats demonstrated a lower the number of times crossing the platform area compared to rats in the healthy group ($p < 0.05$). Compared with CH group, CH+200 AKO and CH+400 AKO-treated rats crossed the platform location more frequently ($p < 0.05$). Therefore, AKO treatment for 50 days obviously improved CH-induced spatial memory impairments (Fig. 1).

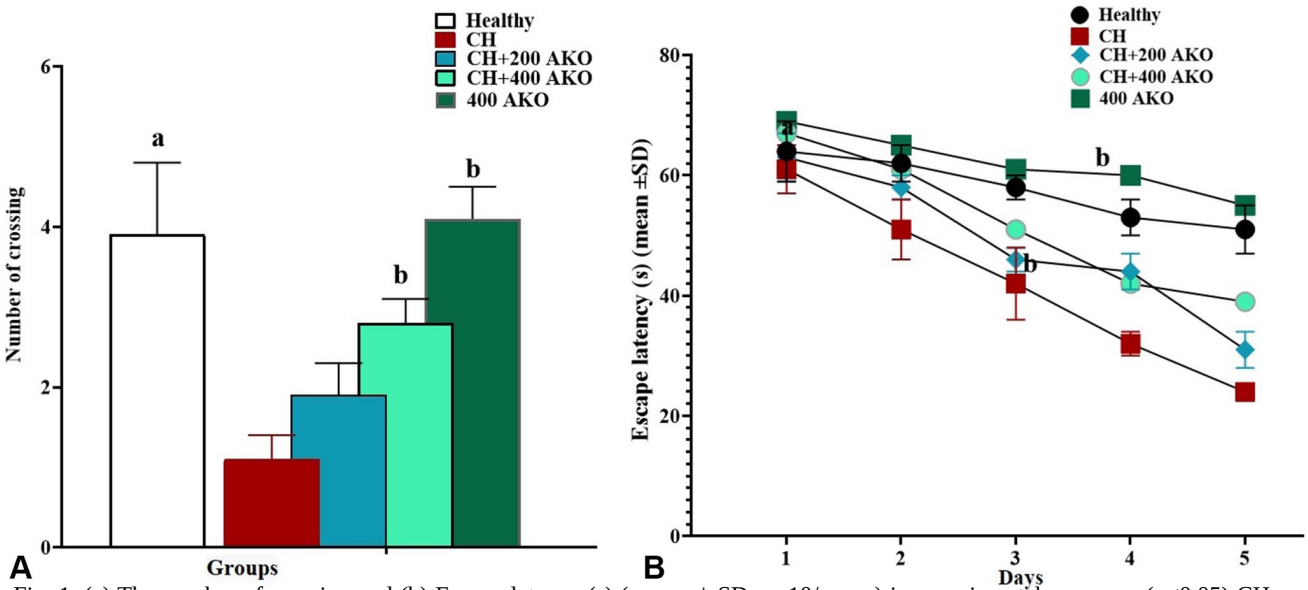

Fig. 1. (a) The number of crossing and (b) Escape latency (s) (means ± SD; n=10/group) in experimental groups. a ($p<0.05$) CH vs. healthy groups; b ($p<0.05$) CH+200 and 400 AKO treated *vs*. CH groups.

Effects of CH and AKO on serum GPx, CAT, and SOD activity alongside serum NO levels. CH, by triggering the generation of free radicals, led to a significant rise in the serum NO concentrations when compared to the healthy group. In contrast, AKO exhibited a dose-dependent reduction in its concentrations in comparison with the CH group. This decrease was statistically significant ($p < 0.05$) in the 400 mg/kg dosage (within the CH+400 AKO group). Furthermore, CH markedly lowered the serum activity of all three antioxidant enzymes in comparison with the healthy rats. Conversely, AKO boosted the serum concentrations of all three enzymes dose-dependently in comparison to the controls, with a significant increase ($p < 0.05$) observed at the 400 mg/kg dosage (within the CH+400 AKO group) compared to the CH group (Fig. 2a).

Effects of CH and AKO on brain thiol, FRAP, and TBARS levels. Thiol, FRAP, and TBARS levels served as key markers of overall antioxidant capacity and LPO. The findings indicated that CH notably ($p < 0.05$) diminished the levels of all three factors in the tissues compared to the healthy group. In contrast, AKO, attributed to its rich antioxidant properties, demonstrated a dose-dependent elevation in the levels of these factors in comparison to the CH group. This elevation was significant ($p < 0.05$) at the 400 mg/kg dosage (within the CH+400 AKO group) in comparison with the CH group (Fig. 2b).

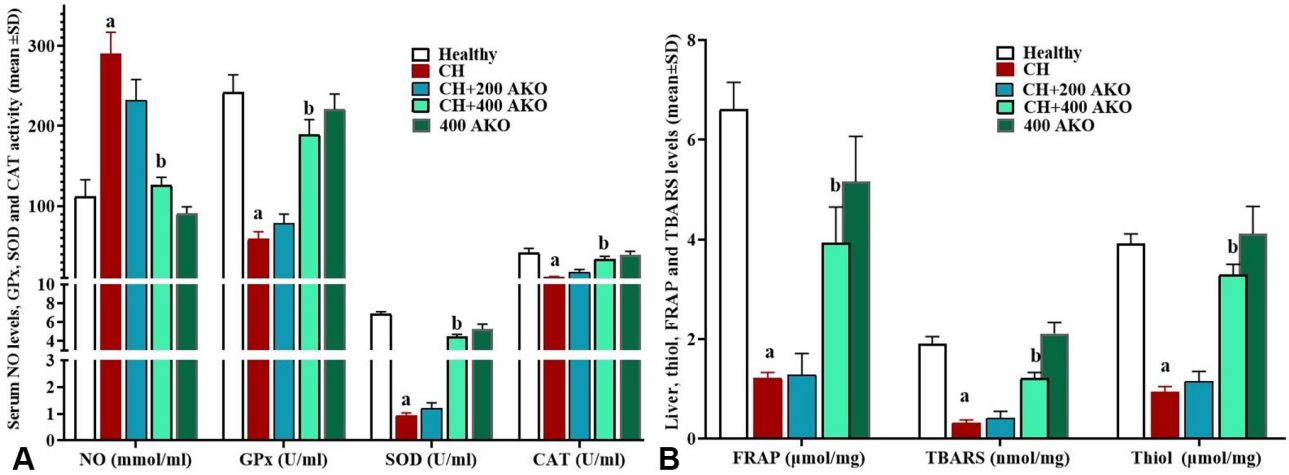

Fig. 2. (a) Serum levels of NO (mmol/ml), alongside the mean serum activity of SOD, CAT, and GPx (U/ml) and (b) Brain tissue levels of TBARS (nmol/mg) and FRAP (µmol/mg) (means ± SD; n=10/group) in experimental groups. [a]($p<0.05$) CH *vs*. healthy groups; [b]($p<0.05$) CH+200 and 400 AKO treated vs. CH groups.

Effects of CH and AKO on serum concentrations of TNF-α, IL-6, IL-10, and IL-1β. By stimulating inflammatory responses, CH increased the concentrations of pro-inflammatory cytokines and suppressed the activity of systemic anti-inflammatory cytokines. This resulted in a significant elevation ($p < 0.05$) in the serum concentrations of all three pro-inflammatory cytokines (TNF-α, IL-1β, and IL-6) in comparison to the healthy group, while the level of IL-10 notably decreased. However, the findings of the study indicated that AKO possesses strong anti-inflammatory properties. It progressively raised the IL-10 serum concentrations and reduced the levels of all three pro-inflammatory cytokines (IL-1β, TNF-α, and IL-6) compared to the AKO group. These changes were significant ($p < 0.05$) at the 400 mg/kg dosage (within the CH+400 AKO group) in comparison to the CH group (Fig. 3).

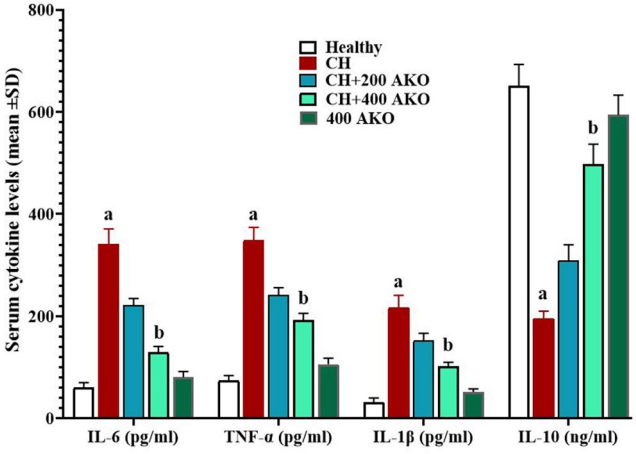

Fig. 3. Serum levels of IL-1β, TNF-α, IL-6 (pg/ml), and IL-10(ng/ml) (means ± SD; n=10/group) in experimental groups. [a]($p<0.05$) CH vs. healthy groups; [b]($p<0.05$) CH+200 and 400 AKO treated *vs.* CH groups.

Effects of CH and AKO on expression of brain TNF-α, IL-6, p53, and IL-1β genes. Analysis of gene expression related to apoptosis pathways revealed that CH treatment significantly increased TNF-α, IL-6, p53, and IL-1β expression in brain compared to the healthy ($p < 0.05$). In the CH+200 AKO group, there was a reduction in TNF-α, IL-6, p53, and IL-1β expression compared with the CH group, however, these alterations were not significant ($p > 0.05$). The most pronounced changes were detected in the CH+400 AKO group where TNF-α, IL-6, p53, and IL-1β expression significantly ($p < 0.05$) increased compared to the CH group (Fig. 4a).

Effects of CH and AKO on expression of brain TNF-α, IL-6, p53, and IL-1β proteins. In order to assess the impact of CH on brain pathways related to apoptosis comprehensively, we investigated the protein expression levels of TNF-α, IL-6, p53, and IL-1β. The findings from

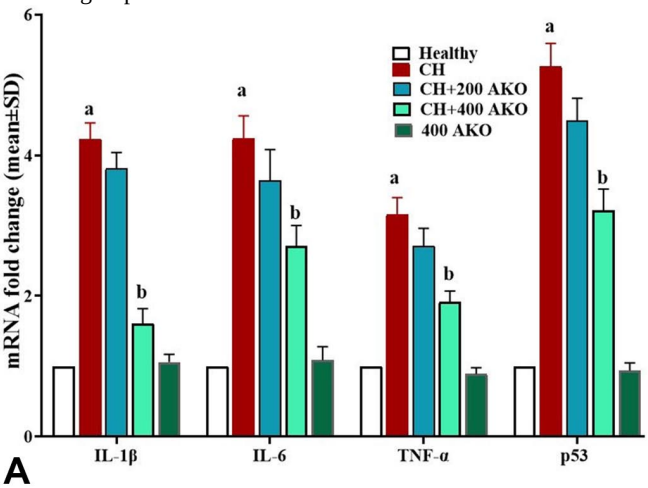

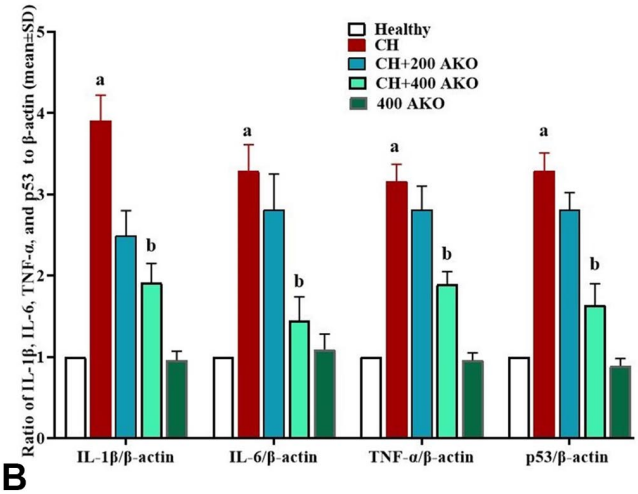

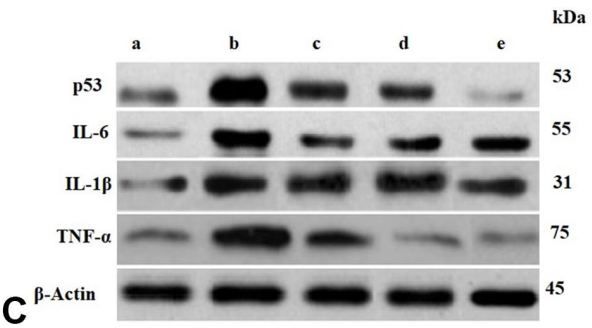

Fig. 4. (a) IL-1β, TNF-α, IL-6, and p53 genes expression and (b) and (c) IL-1β, TNF-α, IL-6, and p53 proteins expression in brain (means ± SD; n=10/group) in healthy (a), CH (b), CH+200 AKO (c), CH+ 400 AKO (d), and 400 AKO (e) groups. a ($p<0.05$) CH vs. healthy groups; b ($p<0.05$) CH+200 and 400 AKO treated vs. CH groups.

this analysis showed a significant increase ($p < 0.05$) in the TNF-α, IL-6, p53, and IL-1β protein expression compared to the healthy group. In contrast, in the CH+200 AKO group, there was a decrease in the protein expression of TNF-α, IL-6, p53, and IL-1β in comparison to the CH group. However, these alterations were not significant ($p > 0.05$). The most notable alterations were observed in the CH+400 AKO group, where there was a significant reduction ($p < 0.05$) in the TNF-α, IL-6, p53, and IL-1β protein expression in comparison with the HCC group (Fig. 4b,c).

Brain p53-positive cells. An analysis of the outcomes concerning the percentage of p53-positive cells indicated that HC led to a notable ($p < 0.05$) rise in the proportion of p53-positive cells in comparison to the healthy group. Furthermore, the groups receiving solely 200 and 400 mg/kg of AKO also exhibited enhancements in the apoptotic indices (decrease in p53-positive cells) when contrasted with the CH group. Particularly, the decrease in the percentage of p53-positive cells in the HC + 400 AKO group was statistically significant in comparison with the HC group (Fig. 5).

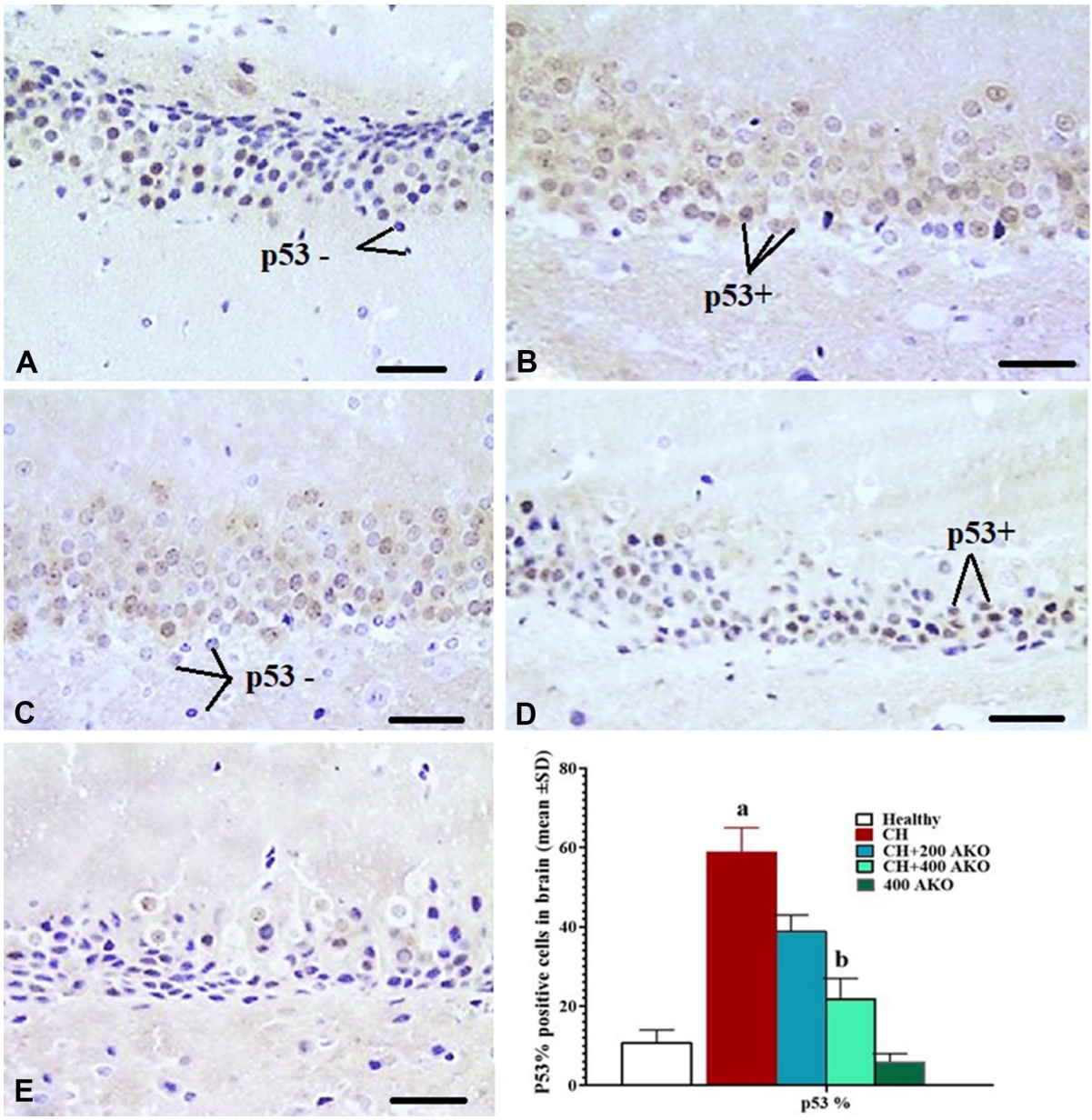

Fig. 5. p53 positive cells (%) in brain tissue by immunohistochemistry (n=10 rat/group, data are "means ± SD) (means ± SD; n=10/group) in healthy (a), CH (b), CH+200 AKO (c), CH+400 AKO (d), and 400 AKO (e) (× 100 with Scale bar = 200 μm). [a] ($p<0.05$) CH *vs*. healthy groups; [b] ($p<0.05$) CH+200 and 400 AKO treated *vs*. CH groups. P53 positive cell (p53+) and p53 negative cell (p53-).

Brain histopathological evaluations. The histopathological analysis of the brain tissue indicated that HC led to the development of lymphocytic infiltration (LI) with vascular lesions (VL), neurons with pyknosis nuclei and vacuolated cytoplasm in the presence of apoptotic bodies, and degenerated neurons (D) near necrotic tissue. In the HC group compared to the normal group, neuronal atrophy occurred in the area and normal parenchyma density showed a significant decrease. While in the treatment groups with AKO, the density of neuronal parenchyma increased and also AKO decreased apoptotic bodies, neuronal degeneration and LI in a dose-dependent manner compared to the HC group (Fig. 6).

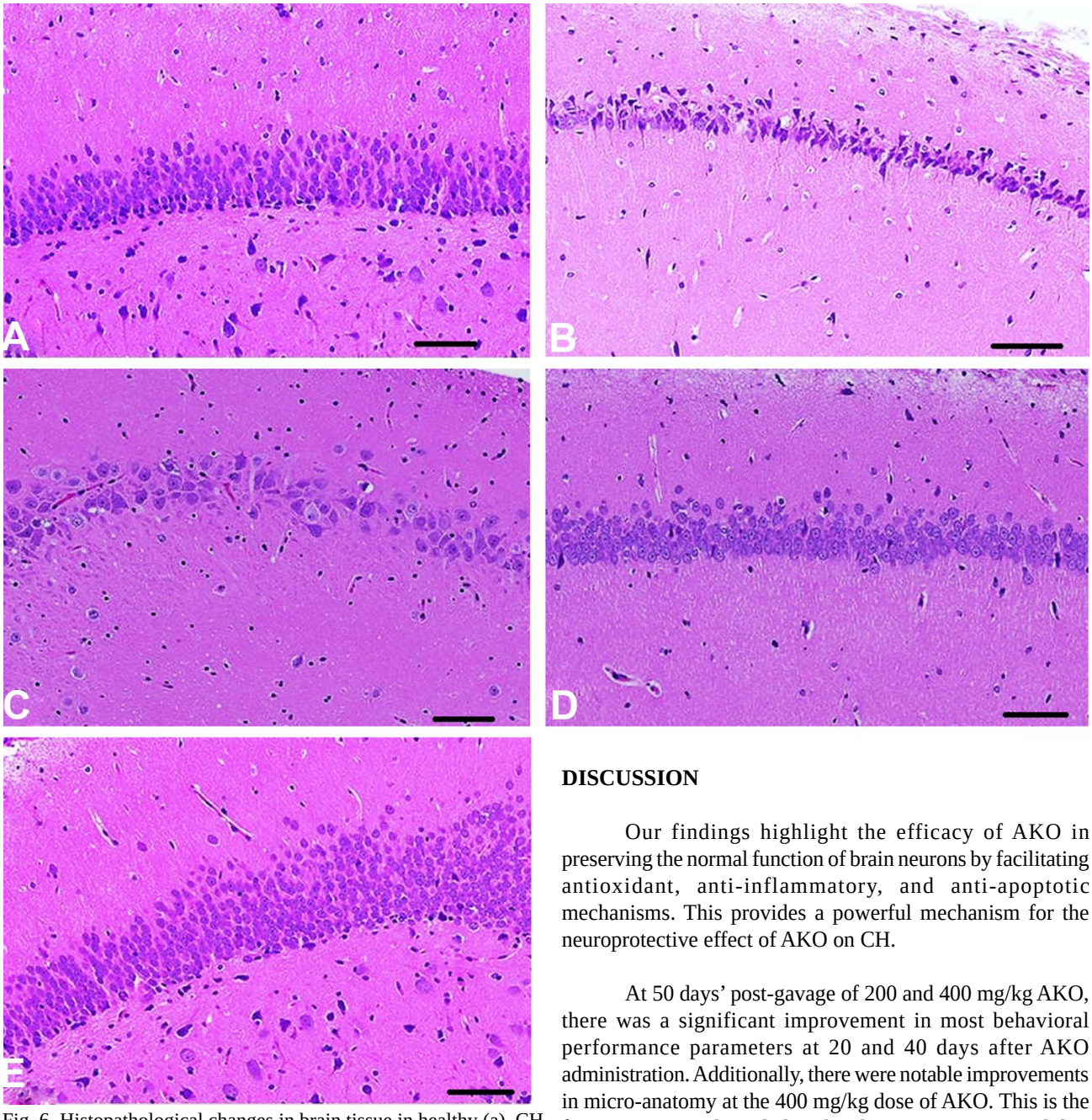

Fig. 6. Histopathological changes in brain tissue in healthy (a), CH (b), CH+200 AKO (c), CH+400 AKO (d), and 400 AKO (e) (× 100 with Scale bar = 200 μm). Histopathological examinations of the brain tissue in the studied groups revealed that CH induced the

DISCUSSION

Our findings highlight the efficacy of AKO in preserving the normal function of brain neurons by facilitating antioxidant, anti-inflammatory, and anti-apoptotic mechanisms. This provides a powerful mechanism for the neuroprotective effect of AKO on CH.

At 50 days' post-gavage of 200 and 400 mg/kg AKO, there was a significant improvement in most behavioral performance parameters at 20 and 40 days after AKO administration. Additionally, there were notable improvements in micro-anatomy at the 400 mg/kg dose of AKO. This is the first report, to our knowledge, that demonstrates AKO's ability to preserve neuron density after a CH, particularly at a dose of 400 mg/kg. When blood flow to a brain region is blocked, nerve impulse transmission from brain neurons is disrupted,

leading to nerve cell degeneration in the affected area, often due to strokes. Research has shown that inflammation and oxidative stress can hinder neuronal plasticity in the hippocampal, resulting in infarct expansion. AKO is known for its anti-inflammatory, anti-apoptosis, and antioxidant properties, as supported by various studies (Akhone *et al*., 2022). It has also been shown that AKO administration inhibits gliosis and counters neuron nucleus destruction in models of arsenic neurotoxicity (Mehram *et al*., 2021). The anti-inflammatory potential of AKO is attributed to flavonoids, while its antioxidant effects are due to flavonoid and phenolic compounds. Vahedi-Mazbadadi *et al*. (2020) demonstrated in an in vitro study that AKO, as an anti-cholinesterase and anti-apoptotic prodrug, exhibited neuroprotective effects and increased the survival of PC12 neurons. Our findings indicate that administering AKO before a CH event can reduce apoptosis area, leading to improved performance in behavioral tests. Genistein, a key flavonoid in AKO, increases GPx and decreases lipid peroxidation by inhibiting the NF-κB pathway in rat brains (Li *et al*., 2022). Furthermore, biochanin A, quercetin, and apigenin have been shown to increase norepinephrine and serotonin levels by modulating oxidative stress in an Alzheimer's model (Jangdey *et al*., 2018; Chiu *et al*., 2023). In our study, we induced CH and evaluated the resulting neurobehavioral changes in rats using various behavioral parameters.

The CH procedure progressively suppressed animal behavior, as evidenced by functional status, neurological impairments, locomotor performance, and exploratory locomotion measured by the Morris water maze test. Pretreating rats with AKO at 200 and 400 mg/kg doses nearly normalized these experimental parameters. Djellal *et al*. (2022), showed that AKO suppresses caspase-9 and cytochrome c, thereby reducing mitochondrial apoptosis and inhibiting neurodegeneration of hippocampal neurons. They also demonstrated that AKO enhances cognitive function related to the striatum and hippocampus through its neuroprotective effects (Djellal *et al*., 2022). In the present study, AKO increased the levels of endogenous antioxidant enzymes by enhancing antioxidant capacity, ultimately decreasing the expression of the p53 gene in hippocampal cells. These beneficial effects of AKO pretreatment suggest it may possess anti-infarct properties. As reported in previous studies, the observed behavioral recovery and reduction in infarct volume may be explained by the preservation of dopaminergic receptors and maintenance of neurotransmitter levels by AKO (Gao *et al*., 2022). However, neurotransmitter levels were not investigated in our study. Further research is needed to elucidate the underlying mechanism of CH in limiting the infarct area. Induction of CH (with collagenase) increases the production of free radicals, resulting in oxidative stress in living organisms. This process can cause membrane lipid peroxidation, leading to loss of membrane integrity and function. Our study demonstrates that AKO possesses neuroprotective properties, as evidenced by preserving neuron density in the hippocampus region. Xing *et al*. (2023) demonstrated that AKO could reduce carbonyl content and lipid peroxidation while improving the concentration of antioxidant enzymes such as superoxide dismutase, catalase, and glutathione, ultimately enhancing the survival rate of rat brain neurons. The increase in neuronal density in the hippocampus after AKO administration is achieved through the inactivation of inflammatory mediators by AKO. The interaction between the CH and hippocampus regions among the injured groups further demonstrated that AKO could enhance hippocampal nerve cell activity by maintaining synaptic plasticity between neurons to replace the damaged area. As a result, AKO improved animal movement performance and reduced the infarct area by promoting neuronal recovery in the hippocampus region. As previously mentioned, quercetin, genistein, and apigenin glycosides are the active components of AKO, and evidence suggests that the neuroprotective effect of AKO treatment correlates with tissue concentrations of FRAP and TBARS levels and serum GPx, CAT, and SOD levels.

CONCLUSION

In conclusion, our study demonstrates that administering AKO before a CH event can reduce hemorrhage volume and improve behavioral performance in rats. The observed neuroprotective effects of AKO may be attributed to its anti-inflammatory, anti-apoptotic, and antioxidant properties, primarily due to flavonoids and other phenolic compounds. Our findings suggest that administering AKO at a dose of 400 mg/kg is particularly effective in preserving neuron density in the hippocampus and reducing CH volume. These results provide valuable insights into the potential application of AKO as a natural therapeutic agent for stroke treatment. Further research is necessary to elucidate the underlying mechanisms of AKO in limiting CH and apoptosis areas and promoting neuronal recovery. Our study highlights the importance of exploring natural compounds like AKO to develop novel CH therapies.

Ethical Approval. The experimental protocols of this study were approved by the Xi'an TCM hospital of encephalopathy ethics committee.

HONG, D.; BI, L.; QIANG, F.; CHEN, X. y QIANG, W. Efectos del extracto de aceite de semilla de albaricoque sobre la función cognitiva y el perfil de expresión de factores inflamatorios en un modelo de accidente cerebrovascular hemorrágico en ratas: un enfoque bioquímico, inmunohistoquímico y molecular. *Int. J. Morphol., 42(5)*:1312-1321, 2024.

RESUMEN: La hemorragia cerebral (HC) presenta un riesgo

significativo de deterioro cognitivo. Nuestra investigación tuvo como objetivo evaluar el impacto del aceite de semilla de albaricoque (ASA) en la función cognitiva y la respuesta inflamatoria en un modelo de accidente cerebrovascular hemorrágico utilizando ratas Wistar, y examinar su correlación. Se asignaron aleatoriamente cincuenta ratas Wistar a cinco grupos: un grupo control, un grupo suplementado con ASA (que recibió 400 mg/kg de ASA), un grupo HC (con HC inducido) y grupos HC suplementados con 200 y 400 mg/kg de ASA, cada uno. La función cognitiva se evaluó mediante la prueba del laberinto eléctrico Y en estos grupos. Además, se utilizaron un ensayo inmunoabsorbente ligado a enzimas y una PCR en tiempo real para analizar los perfiles de expresión de proteínas y genes de factores inflamatorios y apoptóticos en el cerebro. En comparación con el grupo de control, las ratas del grupo HC tardaron más en dominar los criterios del laberinto (P<0,05). Además, el grupo HC exhibió niveles significativamente mayores de citocinas proinflamatorias interleucina-1β (IL-1β), IL-6 y factor de necrosis tumoral-α, y niveles reducidos de citocinas antiinflamatorias IL-4 e IL-10 en comparación al grupo control (P<0,05). Por el contrario, las ratas del grupo HC+400 mg/kg ASA mostraron tendencias opuestas en el tiempo de simulación eléctrica, la proteína del factor inflamatorio y el perfil de expresión génica (Bcl-2, BAX, Caspasa-3 y p53) en comparación con el grupo HC (P <0,05). Nuestros hallazgos sugieren que el extracto de ASA puede mejorar la disfunción cognitiva después de la HC en ratas, potencialmente mediante la modulación de factores inflamatorios secretados por la microglia.

PALABRAS CLAVE: Aceite de semilla de albaricoque; Inflamación; Apoptosis; Hemorragia cerebral.

REFERENCES

Akhone, M. A.; Bains, A.; Tosif, M. M.; Chawla, P.; Fogarasi, M. & Fogarasi, S. Apricot kernel: Bioactivity, characterization, applications, and health attributes. *Foods, 11(15)*:2184, 2022.

Charalabopoulos, A.; Davakis, S.; Lambropoulou, M.; Papalois, A.; Simopoulos, C. & Tsaroucha, A. Apigenin exerts anti-inflammatory effects in an experimental model of acute pancreatitis by down-regulating TNF-α. *In Vivo, 33(4)*:1133-41, 2019.

Chiu, Y. J.; Teng, Y. S.; Chen, C. M.; Sun, Y. C.; Hsieh-Li, H. M.; Chang, K. H. & Lee-Chen, G. J. A neuroprotective action of quercetin and apigenin through inhibiting aggregation of Ab and activation of TRKB signaling in a cellular experiment. *Biomol. Ther. (Seoul), 31(3)*:285-97, 2023.

Deng, H. J.; Zhou, C. H.; Huang, L. T.; Wen, L. B.; Zhou, M. L. & Wang, C. X. Activation of silent information regulator 1 exerts a neuroprotective effect after intracerebral hemorrhage by deacetylating NF-kB/p65. *J. Neurochem., 157(3)*:574-85, 2021.

Djellal, D.; Haddad, S.; Gasmi, S.; Chouit, Z.; Kebieche, M.; Hachemi, M.; Hanfer, M.; Ferhat, N.; Bennoune, O.; Fetoui, H.; *et al*. Chronic thiacloprid exposure impairs cognitive function and triggers mitochondrial apoptosis pathway in rat striatum and hippocampus: neuropreventive effect of bitter apricot kernels extract (*Prunus armeniaca* l.). *J. Microbiol. Biotechnol. Food Sci., 12(3)*:e9089, 2022.

Duan, T.; Li, L.; Yu, Y.; Li, T.; Han, R.; Sun, X.; Cui, Y.; Liu, T.; Wang, X.; Wang, Y.; *et al*. Traditional Chinese medicine use in the pathophysiological processes of intracerebral hemorrhage and comparison with conventional therapy. *Pharmacol. Res., 179*:106200, 2022.

Fouad, A. A.; Abdel-Aziz, A. M. & Hamouda, A. A. Diacerein downregulates NLRP3/Caspase-1/IL-1b and IL-6/STAT3 pathways of inflammation and apoptosis in a rat model of cadmium testicular toxicity. *Biol. Trace Elem. Res., 195(2)*:499-505, 2020.

Gao, L.; Yang, L.; Guo, L.; Wang, H.; Zhao, Y.; Xie, J. & Shi, N. Improving the solubility of melanin nanoparticles from apricot kernels is a potent drug delivery system. *J. Appl. Biomater. Funct. Mater., 20*:22808000221124418, 2022.

Gomaa, E. Z. In vitro antioxidant, antimicrobial, and antitumor activities of bitter almond and sweet apricot (*Prunus armeniaca* L.) kernels. *Food Sci. Biotechnol., 22*:455-63, 2013.

Hassan, M. I.; Ali, F. E. & Shalkami, A. G. S. Role of TLR-4/IL-6/TNF-a, COX-II and eNOS/iNOS pathways in the impact of carvedilol against hepatic ischemia reperfusion injury. *Hum. Exp. Toxicol., 40(8)*:1362-73, 2021.

Jaafar, H. J. Effects of apricot and apricot kernels on human health and nutrition: a review of recent human research. *Technium BioChemMed, 2(2)*:139-62, 2021.

Jangdey, M. S.; Gupta, A. & Sarwa, K. Apigenin and quercetin: potential therapeutic challenging effective against in Alzheimer's disease. *Pharm. Biosci. J.*, 46-51, 2018.

Li, Y.; Zhang, J. J.; Chen, R. J.; Chen, L.; Chen, S.; Yang, X. F. & Min, J. W. Genistein mitigates oxidative stress and inflammation by regulating Nrf2/HO-1 and NF-kB signaling pathways in hypoxic-ischemic brain damage in neonatal mice. *Ann. Transl. Med., 10(2)*:32, 2022.

Magid-Bernstein, J.; Girard, R.; Polster, S.; Srinath, A.; Romanos, S.; Awad, I. A. & Sansing, L. H. Cerebral hemorrhage: pathophysiology, treatment, and future directions. *Circ. Res., 130(8)*:1204-29, 2022.

Mehram, E. B.; Aboraya, A. O. & Elhassaneen, Y. A. E. Potential effects of food processing byproducts on neurological and immunological disorders of obese rats. *Alex. Sci. Exch. J., 42(2)*:509-22, 2021.

Tian, H.; Yan, H.; Tan, S.; Zhan, P.; Mao, X.; Wang, P. & Wang, Z. Apricot kernel oil ameliorates cyclophosphamide-associated immunosuppression in rats. *Lipids, 51(8)*:931-9, 2016.

Tsai, H. J.; Shih, C. C.; Chang, K. Y.; Liao, M. H.; Liaw, W. J.; Wu, C. C. & Tsao, C. M. Angiotensin-(1-7) treatment blocks lipopolysaccharide-induced organ damage, platelet dysfunction, and IL-6 and nitric oxide production in rats. *Sci. Rep., 11(1)*:610, 2021.

Vahedi-Mazdabadi, Y.; Karimpour-Razkenari, E.; Akbarzadeh, T.; Lotfian, H.; Toushih, M.; Roshanravan, N.; Saeedi, M. & Ostadrahimi, A. Anti-cholinesterase and Neuroprotective Activities of Sweet and Bitter Apricot Kernels (*Prunus armeniaca* L.). *Iran. J. Pharm. Res., 19(4)*:216-24, 2020.

Wang, S.; Zou, X. L.; Wu, L. X.; Zhou, H. F.; Xiao, L.; Yao, T.; Zhang, Y.; Ma, J.; Zeng, Y. & Zhang, L. Epidemiology of intracerebral hemorrhage: A systematic review and meta-analysis. *Front. Neurol., 13*:915813, 2022.

Wang, Z.; Jiang, X.; Zhang, L. & Chen, H. Protective effects of Althaea officinalis L. extract against N-diethylnitrosamine-induced hepatocellular carcinoma in male Wistar rats through antioxidative, anti-inflammatory, mitochondrial apoptosis and PI3K/Akt/mTOR signaling pathways. *Food Sci. Nutr., 11(8)*:4756-72, 2023.

Xing, Y. G.; Ding, J. & Guo, L. Acid compounds and nutritional quality of apricot seed kernels from Southern Xinjiang. *Food Sci., 44(12)*:199-207, 2023.

Zeng, J.; Zheng, S.; Chen, Y.; Qu, Y.; Xie, J.; Hong, E.; Lv, H.; Ding, R.; Feng, L. & Xie, Z. Puerarin attenuates intracerebral hemorrhage-induced early brain injury possibly by PI3K/Akt signal activation-mediated suppression of NF-kB pathway. *J. Cell. Mol. Med., 25(16)*:7809-24, 2021.

Zhang, A.; Pan, W.; Lv, J. & Wu, H. Protective effect of amygdalin on LPS-induced acute lung injury by inhibiting NF-kB and NLRP3 signaling pathways. *Inflammation, 40(3)*:745-51, 2017a.

Zhang, X.; Zheng, W.; Wang, T.; Ren, P.; Wang, F.; Ma, X.; Wang, J. & Huang, X. Danshen-Chuanxiong-Honghua ameliorates cerebral impairment and improves spatial cognitive deficits after transient focal ischemia and identification of active compounds. *Front. Pharmacol., 8*:452, 2017b.

Corresponding author:
Dr. Weiping Qiang
Two departments of encephalopathy
Xi'an TCM Hospital of Encephalopath
Xi'an 710032
CHINA

E-mail: 780120qwp@sina.com

ORCID ID: 0009-0004-2226-1401.